Semileptonic $B^- \to \pi^+\pi^-\ell^-\bar{\nu}_\ell$ decay over the full $\pi\pi$ invariant mass spectrum*

Yan-Li Wang (王艳丽)[1†] Xiao-Yu Hao[1‡] Yu-Kuo Hsiao (萧佑国)[1§]

[1]School of Physics and Electronic Engineering, Shanxi Normal University, Taiyuan 030031, China

Abstract: The Belle Collaboration has recently reported a measurement of the branching fraction for the semileptonic decay $B^- \to \pi^+\pi^-\ell^-\bar{\nu}_\ell$, with $\ell = e$ or μ. Using the newly available data across the full $\pi\pi$ invariant-mass spectrum, we determine the non-resonant $B \to \pi\pi$ transition form factors. We obtain a non-resonant branching fraction $\mathcal{B}_N(B^- \to \pi^+\pi^-\ell^-\bar{\nu}_\ell) = (3.5 \pm 1.4^{+4.3}_{-2.4}) \times 10^{-5}$. This result indicates that the non-resonant contribution can be comparable in magnitude to the resonant components and should not be treated as a negligible background in precision measurements. Our findings highlight the importance of dedicated experimental efforts at Belle II and LHCb to further probe the non-resonant contribution.

DOI: 10.1088/1674-1137/ae68ee **CSTR:**

I. INTRODUCTION

Semileptonic b-hadron decays provide an ideal platform for testing heavy-to-light transition form factors [1–6]. Mediated by the quark-level $b \to u\ell\bar{\nu}_\ell$ weak transition, they offer one of the most reliable avenues for determining the Cabibbo–Kobayashi–Maskawa (CKM) matrix element $|V_{ub}|$ [7–15], a key parameter that governs the overall magnitude of CP violation in the Standard Model. Moreover, owing to their relatively small hadronic uncertainties, these decays provide a sensitive probe for potential contributions from physics beyond the Standard Model [16–18].

The four-body decay channel $B \to \pi\pi\ell\bar{\nu}_\ell$ is among the semileptonic B decays that have been measured experimentally [19–23]. In this process, the quasi-two-body contribution $B \to \rho\ell\bar{\nu}_\ell$, followed by the decay $\rho \to \pi\pi$, plays a dominant role. Accordingly, this decay has been extensively studied within various theoretical frameworks, including factorization approaches [24–27], QCD light-cone sum rules [28–33], lattice QCD [34], model-independent parameterizations [35], and phenomenological analyses [36]. However, the nonresonant contribution to $B \to \pi\pi\ell\bar{\nu}_\ell$ represents a genuine four-body decay topology but is often treated as a negligible background and has received comparatively little attention.

The Belle Collaboration has recently measured the branching fractions of $B^- \to \pi^+\pi^-\ell^-\bar{\nu}_\ell$ over the full $\pi\pi$ invariant-mass ($M_{\pi\pi}$) spectrum, as reported in [23].

$$\mathcal{B}_{\rm T}(B^- \to \pi^+\pi^-\ell^-\bar{\nu}_\ell) = (22.7^{+1.9}_{-1.6} \pm 3.5) \times 10^{-5}, \quad (1)$$

with $\ell^- = e^-$ or μ^-. Here, the total branching fraction $\mathcal{B}_{\rm T}$ includes contributions from resonant processes of the form $B^- \to R\ell^-\bar{\nu}_\ell$ followed by $R \to \pi^+\pi^-$, with $R = \rho^0$ or $R = f_2 \equiv f_2(1270)$. Because the $\pi\pi$ invariant-mass spectrum is measured over the full kinematic range, potential non-resonant contributions are also expected. However, a dedicated statistical analysis of the non-resonant component has not yet been performed. Assuming $\mathcal{B}_{\rm T} \simeq \mathcal{B}_\rho + \mathcal{B}_{f_2} + \mathcal{B}_{\rm N}$, where $\mathcal{B}_\rho(B^- \to \rho^0\ell^-\bar{\nu}_\ell, \rho^0 \to \pi^+\pi^-) = (15.8 \pm 1.1) \times 10^{-5}$ [15] and $\mathcal{B}_{f_2}(B^- \to f_2\ell^-\bar{\nu}_\ell, f_2 \to \pi^+\pi^-) = (1.8 \pm 0.9^{+0.2}_{-0.1}) \times 10^{-5}$ [37], the non-resonant branching fraction can be estimated as $\mathcal{B}_{\rm N}(B^- \to \pi^+\pi^-\ell^-\bar{\nu}_\ell) \sim O(10^{-5})$. This indicates that the non-resonant contribution is comparable in magnitude to the resonant components and should not be regarded as a negligible background, thereby warranting dedicated investigation.

The non-resonant decay channel $B^- \to \pi^+\pi^-\ell^-\bar{\nu}_\ell$ is governed by the $B \to \pi\pi$ non-resonant form factors, denoted $F_{\pi\pi}$. Notably, the non-leptonic B decay channel $B^- \to \pi^-\pi^+\pi^-$ also requires $F_{\pi\pi}$ to account for its sizable non-resonant contribution [15], although these form factors remain poorly determined. Currently, little information is available in the literature [7, 24–43]. This

Received 10 April 2026; Accepted 30 April 2026

* This work was supported in part by the National Natural Science Foundation of China (Grant Nos. 12575101 and 12175128)

† E-mail: ylwang0726@163.com

‡ E-mail: 2428405524@qq.com

§ E-mail: yukuohsiao@gmail.com

situation motivates us to extract $F_{\pi\pi}$ from the measured $\pi\pi$ invariant-mass distribution in $B^- \to \pi^+\pi^-\ell^-\bar{\nu}_\ell$. To this end, we will separate the resonant contributions from the non-resonant component and perform a numerical analysis of the branching fractions and angular distributions. In addition, we will examine the sensitivity of the current data to the CKM matrix element $|V_{ub}|$.

II. THEORETICAL FRAMEWORK

As depicted in Figs. 1a and 1b, the decay $B^- \to \pi^+\pi^-\ell^-\bar{\nu}_\ell$ proceeds via resonant and non-resonant $B \to \pi\pi$ transitions, respectively, with the lepton pair produced by the emitted W boson. In the measured $M_{\pi\pi}$ spectrum, a dominant peak and a small bump are identified as arising from the processes $B^- \to \rho^0\ell^-\bar{\nu}_\ell$ and $B^- \to f_2\ell^-\bar{\nu}_\ell$, respectively, where the vector meson ρ^0 and the tensor meson f_2 appear as intermediate resonances decaying into $\pi^+\pi^-$. In addition, a non-resonant component is expected to contribute and can, in principle, be extracted from the data. For our analysis, we express the total amplitude of $B^- \to \pi^+\pi^-\ell^-\bar{\nu}_\ell$ as [44]

$$\begin{aligned}\mathcal{M}_{\rm T} &= \mathcal{M}_{\rm N}(B^- \to \pi^+\pi^-\ell\bar{\nu}_\ell) + \mathcal{M}_\rho(B^- \to \rho^0\ell^-\bar{\nu}_\ell, \rho^0 \to \pi^+\pi^-) \\ &\quad + \mathcal{M}_{f_2}(B^- \to f_2\ell^-\bar{\nu}_\ell, f_2 \to \pi^+\pi^-), \\ \mathcal{M}_{\rm N(R)} &= \frac{G_F V_{ub}}{\sqrt{2}}\langle\pi^+\pi^-|\bar{u}\gamma_\mu(1-\gamma_5)b|B^-\rangle_{\rm N(R)}\,\bar{u}_\ell\gamma^\mu(1-\gamma_5)v_\nu,\end{aligned} \tag{2}$$

where the subscripts T, N, and $R = (\rho, f_2)$ denote the total, non-resonant, and resonant contributions, respectively.

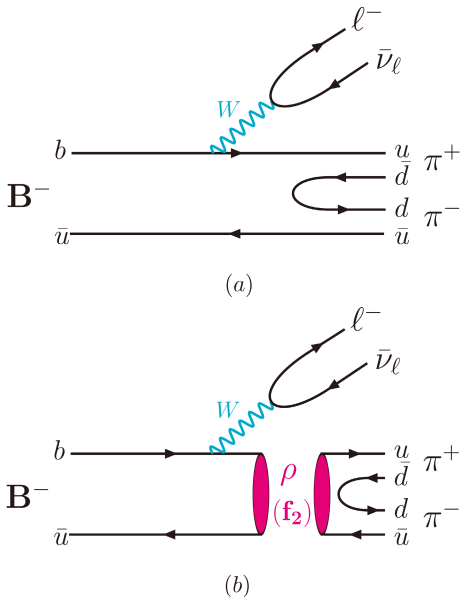

Fig. 1. (color online) Semileptonic $B^- \to \pi^+\pi^-\ell^-\bar{\nu}_\ell$ decay: (a) nonresonant contribution; (b) resonant contributions via the intermediate states ρ^0 and f_2.

The hadronic matrix elements for the (non-)resonant $B \to \pi\pi$ transitions are parameterized as in Refs. [1, 45]

$$\begin{aligned}&\langle\pi^+(p_a)\pi^-(p_b)|\bar{u}\gamma_\mu(1-\gamma_5)b|B^-\rangle_N \\ &= h\epsilon_{\mu\nu\alpha\beta}p_B^\nu p^\alpha(p_b-p_a)^\beta + irq_\mu + iw_+p_\mu + iw_-(p_b-p_a), \\ &\langle\pi^+(p_a)\pi^-(p_b)|\bar{u}\gamma_\mu(1-\gamma_5)b|B^-\rangle_{\rho(f_2)} \\ &= \langle\pi^+\pi^-|\rho(f_2)\rangle\frac{i}{(t-m^2_{\rho(f_2)})+im_{\rho(f_2)}\Gamma_{\rho(f_2)}} \\ &\quad \langle\rho(f_2)|\bar{u}\gamma_\mu(1-\gamma_5)b|B^-\rangle,\end{aligned} \tag{3}$$

where $p = p_b + p_a$, $q = p_B - p = p_\ell + p_\nu$, and $(s,t) \equiv (q^2, p^2)$. The non-resonant form factors are denoted by $F_{\pi\pi} = (h, r, w_\pm)$. The $B \to \rho(f_2)$ transition matrix elements are parameterized as in Refs. [46–48]

$$\begin{aligned}\langle\rho(f_2)|\bar{u}\gamma_\mu b|B\rangle &= \epsilon_{\mu\nu\alpha\beta}\epsilon^{(\prime)\nu}p_B^\alpha p_{\rho(f_2)}^\beta\frac{2V_1^{(\prime)}}{m_B+m_{\rho(f_2)}}, \\ \langle\rho(f_2)|\bar{u}\gamma_\mu\gamma_5 b|B\rangle &= i\left[\epsilon_\mu^{(\prime)} - \frac{\epsilon^{(\prime)}\cdot p_B}{s}q_\mu\right](m_B+m_{\rho(f_2)})A_1^{(\prime)} \\ &\quad + i\frac{\epsilon^{(\prime)}\cdot p_B}{s}q_\mu(2m_{\rho(f_2)})A_0^{(\prime)} \\ &\quad - i\left[(p_B+p_{\rho(f_2)})_\mu - \frac{m_B^2-m_{\rho(f_2)}^2}{s}q_\mu\right] \\ &\quad \times(\epsilon^{(\prime)}\cdot p_B)\frac{A_2^{(\prime)}}{m_B+m_{\rho(f_2)}},\end{aligned} \tag{4}$$

where $\epsilon'^\mu \equiv \epsilon^{\mu\nu}p_{B\nu}/m_B$. Here, ϵ^ν and $\epsilon^{\mu\nu}$ denote the polarization vector and tensor, respectively, and $F_{\rho(f_2)} = (V_1^{(\prime)}, A_{0,1,2}^{(\prime)})$ collects the corresponding transition form factors. The strong decay vertices $\langle\pi\pi|\rho, f_2\rangle$ are given in Refs. [10, 50, 51]

$$\begin{aligned}\langle\pi\pi|\rho\rangle &= g_1\epsilon\cdot(p_b-p_a), \\ \langle\pi\pi|f_2\rangle &= g_2\epsilon^{\mu\nu}p_{a\mu}p_{b\nu},\end{aligned} \tag{5}$$

where $g_{1,2}$ denote strong coupling constants. To perform the sums over the vector and tensor polarizations of the intermediate ρ and f_2 states, we follow Refs. [46–48].

$$\begin{aligned}\Sigma\epsilon_\mu\epsilon^*_{\mu'} &= M_{\mu\mu'}, \\ \Sigma\epsilon_{\mu\nu}\epsilon^*_{\mu'\nu'} &= \frac{1}{2}M_{\mu\mu'}M_{\nu\nu'} + \frac{1}{2}M_{\mu\nu'}M_{\nu\mu'} - \frac{1}{3}M_{\mu\nu}M_{\mu'\nu'},\end{aligned} \tag{6}$$

with $M_{\mu\mu'} = -g_{\mu\mu'} + p_\mu p_{\mu'}/p^2$. The form factors in Eqs. (3) and (4) are momentum-dependent and are modeled using either single- or double-pole parametrizations [46–48]:

$$F_\rho(s) = \frac{F_\rho(0)}{1 - s/m_V^2},$$
$$F_{f_2}(s) = \frac{F_{f_2}(0)}{(1 - s/m_B^2)^2}, \quad (7)$$
$$F_{\pi\pi}(t) = \frac{F_{\pi\pi}(0)}{1 - a(t/m_B^2) + b(t/m_B^2)^2},$$

where F_ρ and F_{f_2} have been studied within QCD-based approaches [48, 49], while the parameters $(a, b, F_{\pi\pi}(0))$ are extracted from a global fit.

For the four-body decay channel $B^-(p_B) \to \pi^+(p_a)\pi^-(p_b)\ell^-(p_\ell)\bar{\nu}_\ell(p_\nu)$, the phase-space integration is performed over the kinematic variables $(s, t, \theta_M, \theta_L, \phi)$. As illustrated in Fig. 2, $\theta_{M(L)}$ denotes the angle between the momenta of the π^+ and π^- (of the ℓ^- and $\bar{\nu}_\ell$) in the $\pi^+\pi^-$ ($\ell^-\bar{\nu}_\ell$) rest frame. In addition, the angle ϕ is defined as the angle between the decay planes of the $\pi^+\pi^-$ and $\ell^-\bar{\nu}_\ell$ systems, which are formed by $\vec{p}_{a,b}$ and $\vec{p}_{\ell,\bar{\nu}_\ell}$, respectively, in the B-meson rest frame. The differential decay width is given by [1, 3, 4]

$$d\Gamma = \frac{|\mathcal{M}|^2}{4(4\pi)^6 m_B^3} X \alpha_M \alpha_L \, ds\, dt\, d\cos\theta_M\, d\cos\theta_L\, d\phi, \quad (8)$$

where X, α_M, and α_L are defined as in [43, 52, 53]

$$X = \left[\frac{1}{4}(m_B^2 - s - t)^2 - st\right]^{1/2},$$
$$\alpha_M = \frac{1}{t}\lambda^{1/2}(t, m_\pi^2, m_\pi^2),$$
$$\alpha_L = \frac{1}{s}\lambda^{1/2}(s, m_\ell^2, m_{\bar{\nu}}^2), \quad (9)$$

With $\lambda(a,b,c) = a^2 + b^2 + c^2 - 2ab - 2bc - 2ca$. The allowed ranges for (s,t) and the angular variables $(\theta_M, \theta_L, \phi)$ are:

$$(m_\ell + m_{\bar{\nu}_\ell})^2 \le s \le (m_B - \sqrt{t})^2, \; 4m_\pi^2 \le t \le (m_B - m_\ell - m_{\bar{\nu}_\ell})^2,$$
$$0 \le \theta_{M,L} \le \pi, \; 0 \le \phi \le 2\pi, \quad (10)$$

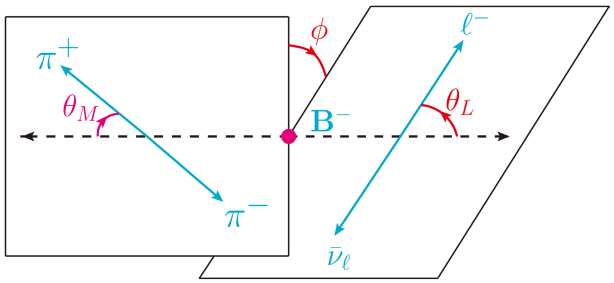

Fig. 2. (color online) The angular variables $(\theta_M, \theta_L, \phi)$ in the four-body $B^- \to \pi^+\pi^-\ell^-\bar{\nu}_\ell$ decay.

With $m_\ell + m_{\bar{\nu}_\ell} \simeq 0$, the angular asymmetry is defined from Eq. (8), as in Refs. [54–56].

$$A_{\theta_M} \equiv \frac{\int_0^{+1} \frac{d\Gamma}{d\cos\theta_M} d\cos\theta_M - \int_{-1}^{0} \frac{d\Gamma}{d\cos\theta_M} d\cos\theta_M}{\int_0^{+1} \frac{d\Gamma}{d\cos\theta_M} d\cos\theta_M + \int_{-1}^{0} \frac{d\Gamma}{d\cos\theta_M} d\cos\theta_M}, \quad (11)$$

where $d\Gamma/d\cos\theta_M$ represents the angular distribution.

III. NUMERICAL ANALYSIS

In the numerical analysis, we perform a minimum χ^2 fit to extract, as free parameters, $|V_{ub}|$, the nonresonant form factors $F_{\pi\pi}$, and $\delta_{1,2}$, where $\delta_{1(2)}$ denotes the relative phase associated with $\mathcal{M}_{\rho(f_2)}$. The χ^2 function is defined as

$$\chi^2 = \left(\frac{\mathcal{B}_{\rho th} - \mathcal{B}_{\rho ex}}{\sigma_{\rho ex}}\right)^2 + \left(\frac{\mathcal{B}_{f_2 th} - \mathcal{B}_{f_2 ex}}{\sigma_{f_2 ex}}\right)^2$$
$$+ \sum_i \left(\frac{\frac{d\mathcal{B}^i_{th}}{dM_{\pi\pi}} - \frac{d\mathcal{B}^i_{ex}}{dM_{\pi\pi}}}{\sigma^i_{ex}}\right)^2 + \sum_j \left(\frac{F^j_\rho - F^j_{th\rho}}{\delta F^j_{th\rho}}\right)^2$$
$$+ \sum_k \left(\frac{F^k_{f_2} - F^k_{th\, f_2}}{\delta F^k_{th\, f_2}}\right)^2, \quad (12)$$

where $d\mathcal{B}/dM_{\pi\pi}$ denotes the differential branching fraction, and σ_{ex} (δF_{th}) represents the experimental (theoretical form-factor) uncertainty. The theoretical inputs $\mathcal{B}_{\rho(f_2)th}$ and $d\mathcal{B}_{th}/dM_{\pi\pi}$ are obtained from the amplitudes in Eq. (2), whereas the experimental inputs are taken from Eq. (1) and Fig. 3. We use $F_\rho^{(j)} = (V_1(0), A_1(0), A_2(0))$ and $F_{f_2}^{(k)} = (V_1'(0), A_1'(0), A_2'(0))$ from Table 1 as input values for Eq. (12), together with $|g_1| = 5.98$ and $|g_2| = 18.56$ in units of GeV^{-1} [51, 57].

From the fit, we obtain

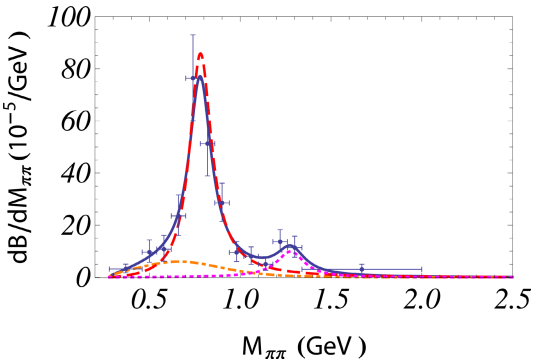

Fig. 3. (color online) The $\pi\pi$ invariant-mass spectrum. The solid curve includes all contributions and reproduces the data points from Belle [23]. The dashed (dotted) curve represents the contributions from $B^- \to \rho(f_2)\ell\bar{\nu}$, with $\rho(f_2) \to \pi^+\pi^-$, while the dot-dashed curve denotes the nonresonant contribution.

Table 1. We parameterize the $B\to(\rho,f_2)$ transition form factors using the pole mass $M_V=7.0$ GeV as given in Eq. (7) [48, 49]. Here, we adopt the isospin relation $\sqrt{2}F_{\rho^0}=F_\rho$ for the $B\to\rho^0$ transition.

	$V_1^{(\prime)}$	$A_1^{(\prime)}$	$A_2^{(\prime)}$
$\sqrt{2}F_{\rho^0}(0)$	$0.35^{+0.06}_{-0.05}$	$0.27^{+0.05}_{-0.04}$	$0.26^{+0.05}_{-0.03}$
$F_{f_2}(0)$	(0.18 ± 0.02)	(0.13 ± 0.02)	(0.12 ± 0.02)

$$
\begin{aligned}
&|V_{ub}|=(3.31\pm0.61)\times10^{-3},\\
&a=(26.8\pm25.9),\ b=(1430.1\pm680.1),\\
&h(0)=(1.90\pm0.43)\ \text{GeV}^{-3},\\
&w_+(0)=(6.16\pm3.41)\ \text{GeV}^{-1},\ w_-(0)=(3.67\pm1.79)\ \text{GeV}^{-1},\\
&(\delta_1,\delta_2)=(-111.6\pm29.3,0.0\pm1.4)^\circ,\\
&\chi^2/n.d.f.=1.1,
\end{aligned}
\tag{13}
$$

with $n.d.f.=7$ denoting the number of degrees of freedom. We note that the form factor r in Eq. (3) and $A_0^{(\prime)}$ in Eq. (4) do not contribute to the fit, as their contributions to the amplitudes vanish since $q_\mu\bar{u}_\ell\gamma^\mu(1-\gamma_5)v_\nu=0$ for nearly massless leptons.

Using the fitted parameters in Eq. (13), we obtain

$$
\begin{aligned}
&\mathcal{B}_{\rm T}(B^-\to\pi^+\pi^-\ell^-\bar{\nu}_\ell)=(19.6\pm7.9^{+7.5+0.7}_{-5.4-0.1})\times10^{-5},\\
&\mathcal{B}_{\rho}(B^-\to\rho^0\ell^-\bar{\nu}_\ell,\rho^0\to\pi^+\pi^-)=(15.8\pm6.4^{+7.1}_{-5.7})\times10^{-5},\\
&\mathcal{B}_{f_2}(B^-\to f_2\ell^-\bar{\nu}_\ell,f_2\to\pi^+\pi^-)=(2.6\pm1.1^{+1.2}_{-0.9})\times10^{-5},\\
&\mathcal{B}_{\rm N}(B^-\to\pi^+\pi^-\ell^-\bar{\nu}_\ell)=(3.5\pm1.4^{+4.3}_{-2.4})\times10^{-5},
\end{aligned}
\tag{14}
$$

where the first uncertainty arises from $|V_{ub}|$, the second from the form factors, and the third (for $\mathcal{B}_T$) from the phase δ_1. The partial branching fractions as functions of $M_{\pi\pi}$ and $\cos\theta_M$ are shown in Fig. 3 and Fig. 4, respectively. We further evaluate the angular asymmetries using Eq. (11) and obtain

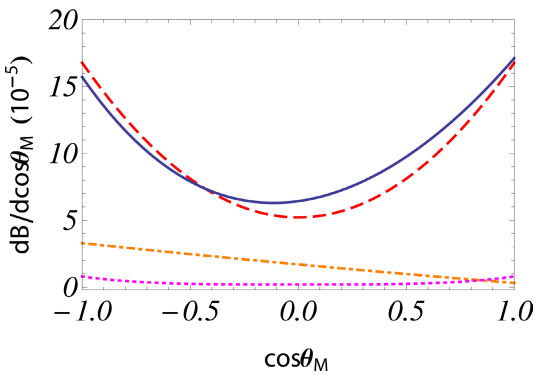

Fig. 4. (color online) Angular distributions for the decay $B^-\to\pi^+\pi^-\ell^-\bar{\nu}_\ell$. The solid, dashed, dotted, and dot-dashed curves represent the same contributions as in Fig. 3

$$
\begin{aligned}
&A_{\theta_M,\rm T}(B^-\to\pi^+\pi^-\ell^-\bar{\nu}_\ell)=(1.3\pm8.9^{+0.8}_{-2.5})\%,\\
&A_{\theta_M,\rho}(B^-\to\rho^0\ell^-\bar{\nu}_\ell,\rho^0\to\pi^+\pi^-)=(0.20\pm0.04)\%,\\
&A_{\theta_M,f_2}(B^-\to f_2\ell^-\bar{\nu}_\ell,f_2\to\pi^+\pi^-)=(0.31\pm0.08)\%,\\
&A_{\theta_M,\rm N}(B^-\to\pi^+\pi^-\ell^-\bar{\nu}_\ell)=(-43.0\pm22.3)\%,
\end{aligned}
\tag{15}
$$

where the first set of uncertainties arises from the form factors, and the second (for $A_{\theta_M,\rm T}$) arises from the phase δ_1.

IV. DISCUSSIONS AND CONCLUSIONS

We investigate the four-body decay channel $B^-\to\pi^+\pi^-\ell^-\bar{\nu}_\ell$ by performing a global fit to the $M_{\pi\pi}$ invariant mass spectrum shown in Fig. 3. The resulting $\chi^2/n.d.f.\simeq1$ indicates that our model provides a statistically robust description of the data. By employing the form factors extracted from the global fit (as detailed in Eq. (13)), we present the differential branching fractions $d\mathcal{B}_{(T,\rho,f_2,N)}/dM_{\pi\pi}$ in Fig. 3, illustrating the individual and total contributions to the mass spectrum. The solid curve representing $d\mathcal{B}_T/dM_{\pi\pi}$ is in good agreement with the experimental data. Notably, the non-resonant contribution ($d\mathcal{B}_N/dM_{\pi\pi}$), shown by the dot-dashed curve, plays a critical role in shaping the overall distribution, particularly in the low $M_{\pi\pi}$ region. Our analysis yields the first estimate of the non-resonant branching fraction, $\mathcal{B}_{\rm N}=(3.5\pm1.4^{+4.3}_{-2.4})\times10^{-5}$. This result indicates that $\mathcal{B}_{\rm N}$ can reach the 10^{-5} level and, therefore, should no longer be neglected in precision studies.

The fitted relative phase δ_1 leads to destructive interference involving the resonant process $B^-\to(\rho^0\to)\pi^+\pi^-\ell^-\bar{\nu}_\ell$, an effect that is most prominent in the $M_{\pi\pi}\simeq m_\rho$ region. In contrast, δ_2 is found to be consistent with zero. This reflects the suppression of the non-resonant contribution for $M_{\pi\pi}>1$ GeV, leading to negligible interference with the $B^-\to(f_2\to)\pi^+\pi^-\ell\bar{\nu}$ channel. From the fit results in Eq. (13), we obtain $|V_{ub}|=(3.31\pm0.61)\times10^{-3}$, which is consistent with current determinations. Although the relatively large uncertainty renders this result less competitive than existing extractions reported by the PDG [15], it nevertheless demonstrates that the four-body semileptonic decay $B\to\pi\pi\ell\bar{\nu}$ is sensitive to $|V_{ub}|$. This provides a novel and independent avenue for its determination. Future high-precision measurements will be essential to reduce the experimental uncertainty and fully exploit the potential of this decay channel.

The angular asymmetries provide stringent constraints on the underlying form factors [54–56]. Our analysis, as summarized in Eq. (15), shows that $A_{\theta_M,\rho}$ and

A_{θ_M,f_2} are both approximately zero. Specifically, $A_{\theta_M,\rho}$ exhibits a symmetric distribution, as shown in Fig. 4, while A_{θ_M,f_2} remains nearly flat. By contrast, $A_{\theta_M,\mathrm{N}} \sim -40\%$ displays a clear, decreasing dependence on $\cos\theta_M$. This behavior is dominated by the form factor associated with the structure $w_-(p_b - p_a)$. In the $\pi^+(p_a)\pi^-(p_b)$ rest frame (see Fig. 2), the term $p_b - p_a = (0, 2\vec{p}_b)$ from the w_- contribution projects onto the four-momentum of the lepton-pair system, inducing a pronounced $\cos\theta_M$ dependence. Consequently, future experimental measurements of these angular asymmetries will serve as a powerful tool to test the existence and magnitude of the non-resonant contribution.

In summary, we have investigated the four-body semileptonic decay $B^- \to \pi^+\pi^-\ell\bar{\nu}$. By analyzing the full $\pi\pi$ invariant mass spectrum measured by the Belle Collaboration, we have determined $|V_{ub}| = (3.31 \pm 0.61) \times 10^{-3}$, a value consistent with current determinations. Furthermore, we have extracted the non-resonant $B \to \pi\pi$ transition form factors and predicted the non-resonant branching fraction to be $\mathcal{B}_{\mathrm{N}}(B^- \to \pi^+\pi^-\ell^-\bar{\nu}_\ell) = (3.5 \pm 1.4^{+4.3}_{-2.4}) \times 10^{-5}$. We have also presented the non-resonant angular asymmetry $A_{\theta_M,\mathrm{N}}(B^- \to \pi^+\pi^-\ell^-\bar{\nu}_\ell) = (-43.0 \pm 22.3)\%$. These predictions offer a clear signature of the non-resonant component and can be rigorously tested in future high-precision measurements at Belle II and LHCb.

References

[1] C. L. Y. Lee, M. Lu, M. B. Wise, Phys. Rev. D **46**, 5040 (1992)
[2] D. Becirevic, A. B. Kaidalov, Phys. Lett. B **478**, 417 (2000)
[3] C. Q. Geng, Y. K. Hsiao, Phys. Lett. B **704**, 495 (2011)
[4] C. Q. Geng, Y. K. Hsiao, Phys. Rev. D **85**, 094019 (2012)
[5] P. Gambino, A. S. Kronfeld, M. Rotondo, *et al.*, Eur. Phys. J. C **80**, 966 (2020)
[6] Y. K. Hsiao, Eur. Phys. J. C **83**, 300 (2023)
[7] X. W. Kang, B. Kubis, C. Hanhart, Phys. Rev. D **89**, 053015 (2014)
[8] T. Feldmann, B. Müller, D. van Dyk, *et al.*, Phys. Rev. D **92**, 034013 (2015)
[9] Y. K. Hsiao, C. Q. Geng, Phys. Lett. B **755**, 418 (2016)
[10] C. S. Kim, G. L. Castro, S. L. Tostado, Phys. Rev. D **95**, 073003 (2017)
[11] Y. K. Hsiao, C. Q. Geng, Eur. Phys. J. C **77**, 714 (2017)
[12] Y. K. Hsiao, C. Q. Geng, Phys. Lett. B **782**, 728 (2018)
[13] D. Leljak, B. Melić, F. Novak, *et al.*, JHEP **08**, 063 (2023)
[14] I. Adachi, *et al.*, Phys. Rev. D **111**, 112009 (2025)
[15] S. Navas, *et al.*, Phys. Rev. D **110**, 030001 (2024)
[16] A. Crivellin, Phys. Rev. D **81**, 031301 (2010)
[17] A. J. Buras, K. Gemmler, G. Isidori, Nucl. Phys. B **843**, 107 (2011)
[18] A. Crivellin, S. Pokorski, Phys. Rev. Lett. **114**, 011802 (2015)
[19] B. H. Behrens, *et al.*, Phys. Rev. D **61**, 052001 (2000)
[20] T. Hokuue, *et al.*, Phys. Lett. B **648**, 139 (2007)
[21] A. Sibidanov, *et al.*, Phys. Rev. D **88**, 032005 (2013)
[22] P. del Amo Sanchez, *et al.*, Phys. Rev. D **83**, 032007 (2011)
[23] C. Beleño, *et al.*, Phys. Rev. D **103**, 112001 (2021)
[24] S. Faller, T. Feldmann, A. Khodjamirian, *et al.*, Phys. Rev. D **89**, 014015 (2014)
[25] P. Böer, T. Feldmann, D. van Dyk, JHEP **02**, 133 (2017)
[26] T. Feldmann, D. Van Dyk, K. K. Vos, JHEP **10**, 030 (2018)
[27] B. Grinstein, D. Pirjol, Phys. Rev. D **73**, 094027 (2006)
[28] C. Hambrock, A. Khodjamirian, Nucl. Phys. B **905**, 373 (2016)
[29] S. Descotes-Genon, A. Khodjamirian, J. Virto, JHEP **12**, 083 (2019)
[30] U. G. Mei?ner, W. Wang, Phys. Lett. B **730**, 336 (2014)
[31] S. Cheng, A. Khodjamirian, J. Virto, JHEP **05**, 157 (2017)
[32] S. Cheng, A. Khodjamirian, J. Virto, Phys. Rev. D **96**, 051901 (2017)
[33] S. Cheng, Phys. Rev. D **112**, L111301 (2025)
[34] L. Leskovec, S. Meinel, M. Petschlies, *et al.*, Phys. Rev. Lett. **134**, 161901 (2025)
[35] F. Herren, B. Kubis, R. van Tonder, Phys. Rev. D **112**, 1 (2025)
[36] F. U. Bernlochner, S. Wallner, Phys. Rev. D **109**, 074040 (2024)
[37] C. Beleño, "Measurement of $B \to \pi\pi\ell\bar{\nu}$ with Full Hadronic Reconstruction at Belle," thesis, Gottingen University (2018)
[38] S. Fajfer, R.J. Oakes, T. N. Pham, Phys. Rev. D **60**, 054029 (1999)
[39] C. K. Chua, W. S. Hou, S. Y. Shiau, *et al.*, Phys. Rev. D **67**, 034012 (2003)
[40] C. K. Chua, W. S. Hou, S. Y. Shiau, *et al.*, Eur. Phys. J. C **33**, S253 (2004)
[41] Y. K. Hsiao, S. Y. Tsai, E. Rodrigues, Eur. Phys. J. C **80**, 565 (2020)
[42] S. Cheng, Phys. Rev. D **99**, 053005 (2019)
[43] Y. K. Hsiao, C. Q. Geng, Phys. Lett. B **770**, 348 (2017)
[44] Y. K. Hsiao, Y. L. Wang, W. J. Wei, arXiv:2507.20380[hep-ph]
[45] A. Pais, S. B. Treiman, Phys. Rev. **168**, 1858 (1968)
[46] Y. B. Zuo, C. X. Yue, B. Yu, *et al.*, Eur. Phys. J. C **81**, 30 (2021)
[47] W. Wang, Phys. Rev. D **83**, 014008 (2011)
[48] H. Y. Cheng, K. C. Yang, Phys. Rev. D **83**, 034001 (2011)
[49] L. Del Debbio, *et al.*, Phys. Lett. B **416**, 392 (1998)
[50] H. Y. Cheng, C. K. Chua, Phys. Rev. D **102**, 053006 (2020)
[51] M. Suzuki, Phys. Rev. D **47**, 1043 (1993)
[52] Y. K. Hsiao, Phys. Lett. B **845**, 138158 (2023)
[53] Y. K. Hsiao, S. Q. Yang, W. J. Wei, *et al.*, JHEP **12**, 226 (2025)
[54] X. Huang, Y. K. Hsiao, J. Wang, *et al.*, Phys. Rev. D **105**, 076016 (2022)
[55] Y. K. Hsiao, C. Q. Geng, Phys. Rev. D **93**, 034036 (2016)
[56] C. Q. Geng, Y. K. Hsiao, Phys. Rev. D **74**, 094023 (2006)
[57] Y. K. Hsiao, Y. Yu, B. C. Ke, Eur. Phys. J. C **80**, 895 (2020)